Glacial/interglacial variations of meridional transport and washout of dust: A one-dimensional model

Katrine K. Andersen [1] and Peter D. Ditlevsen

Department of Geophysics, Niels Bohr Institute, University of Copenhagen, Denmark

Abstract. Measurements of $\delta^{18}O$ and insoluble dust in the Greenland Ice Core Project ice core reveal that the concentration of dust is about 100 times higher in ice from the last glacial maximum than it is today. In order to understand the glacial climate it is of importance to establish to what extent this increased level was due to changes in the source areas and to what extent it was due to changes in the atmospheric transportation. We here present a one-dimensional model evaluating the effect of changes in the zonally averaged atmospheric circulation on the atmospheric hydrological cycle and dust transportation. The main characteristics of the altered climate during glacial periods are assumed to be increased baroclinicity, an equatorward displacement of the baroclinic zone, and reduced evaporation. The model reproduces the zonally averaged hydrological cycle of the present climate reasonably well, and it produces a halving of snow accumulation in polar areas for glacial periods. From the ice core data we obtain a power law dependence between the concentration of dust in the ice and the accumulation related to long-term climate variations. With the input of dust to the atmosphere being independent of the simulated climate, the model reproduces this power law. The obtained power is strongly dependent on the assumed position of the dust sources. For reasonable estimates of the present-day dust sources the simulated mechanism may account for a twofold to sixfold increase in dust concentration in polar ice from interglacial to full glacial conditions. Concurrently, the atmospheric content of dust is increased at all latitudes during the glacial period.

1. Introduction

Ice core data reveil a strong connection between the amount of eolian dust deposited on the polar ice sheets and climate variations as recorded by $\delta^{18}O$, the temperature proxy [Hammer et al., 1985; Petit et al., 1981; Thompson and Mosley-Thompson, 1981]. Recently this connection has been quantified by Marsh and Ditlevsen [1997], who for the Greenland Ice Core Project (GRIP) ice core found a strong negative correlation between $\delta^{18}O$ and the calcium concentration, a proxy for continental dust, for timescales longer than ~200 years.

Several circumstances, such as changes in the source areas, increased production due to higher wind speeds over the source areas, and altered transportation routes, may contribute to the increased amounts of eolian dust during cold periods. The sources of dust during glacial periods may have been different from the present ones due to the occurrence of additional arid/semiarid areas, the covering of potential source areas by ice sheets (e.g., the Laurentide ice sheet), and the uncovering of shelf areas as a result of the decreased sea level. From geological records and general circulation models (GCMs), for example [Kutzbach and Wright Jr., 1985], as well as from a statistical analysis of ice core data [Ditlevsen et al., 1996], it appears that the glacial atmosphere was more stormy than the present. This makes an increased uptake of dust plausible. An equatorward displacement of the baroclinic zone during glacial times implies a change of the atmospheric hydrological cycle and a redistribution of the deposition areas of dust. Simultaneously stronger baroclinicity results in higher wind speeds and shorter transportation times across the baroclinic zone. Taken together with a generally decreased precipitation, these factors imply an increased residence time of dust in the atmosphere and a more dusty atmosphere. Three-dimensional (3-D) GCM simulations [Andersen and Genthon, 1996; Genthon, 1992; Joussaume, 1993] did not succeed in reproducing the observed concentrations of dust in glacial ice, and a 2-D model study [Yung et al., 1996] showed that by reducing the washout rate of dust in the atmosphere, an enhancement by a factor 2-3 of dust in Antarctic ice results. This is still a factor of 3 short if

[1] Also at Laboratoire de Glaciologie et Géophysique de l'Environnement, Centre National de la Recherche Scientifique, Saint-Martin-d'Hères Cedex, France

compared with measured data. From a 0-D model considering the influence of altered transit and residence times on the deposition of impurities, [*Hansson*, 1995] found a tenfold increase in the impurity concentration as observed for the Renland ice core. K. Fuhrer et al. (Causes of dust variability in the GRIP (Greenland) ice core in the last 100,000 years, submitted to *Earth and Planetary Science Letters*, 1997) recently discussed the relative importance of the different factors influencing the calcium concentration (representing dust) of the GRIP ice core in the past 100,000 years, differentiating between shorter interstadials and an underlying long-term trend. They ascribed short-term variations to higher wind speeds in the source areas together with increased residence times, caused by decreased precipitation rates, and ascribed long-term trends partly to changes in transportation efficiency connected to the waxing and waning of ice sheets.

In order to estimate the relative importance and order of magnitude of the major mechanisms influencing the amount of dust in polar ice cores, we have constructed a 1-D diffusive model of the transport of moisture and passive tracers from their low- and middle-latitude sources to the polar regions. Results of this model are evaluated by comparison with measurements of Cl⁻ and insoluble dust [*De Angelis et al.*, 1997; *Steffensen*, 1997] obtained from the GRIP ice core drilled at the summit of the Greenland ice cap [*Greenland Ice Core Project members*, 1993].

2. The Model

In the model the climatology is prescribed by the zonally averaged midatmosphere temperature T. The interglacial temperature profile is prescribed from present-day climatology [*Peixeto and Oort*, 1992], and the main difference between the full glacial (FG) and the interglacial (IG) atmosphere is assumed to be a larger equator to ice-rim temperature difference and, for the northern hemisphere, extended ice sheets at high latitudes during glacial periods. This implies a steeper baroclinic zone, which is moved equatorward, as seen in Figure 1a. The temperature difference at 80°N latitude between the two extreme cases, the present climate and the climate of the last glacial maximum (LGM), is taken to be 15°C, in between the maximum value of 22°C suggested by [*Johnsen et al.*, 1995] for the summit of the Greenland ice sheet and earlier lower estimates [*Johnsen et al.*, 1992]. The temperature difference at the equator is taken to be 5°C [*Guilderson et al.*, 1994]. The robustness of the model toward variation of the different parameters described here is discussed in section 3.1.

Atmospheric transportation is described as a diffusion, with a diffusion constant varying latitudinally in proportion with the temperature gradient, $k(\phi) = k'\partial T/\partial\phi$ [*Wiin-Nielsen*, 1988]. With $\mu = \sin\phi$, ϕ being the latitude, a being the Earth radius and all quantities referring to zonal averages, the dynamics for a constituent, $x(\mu,t)$, is determined from
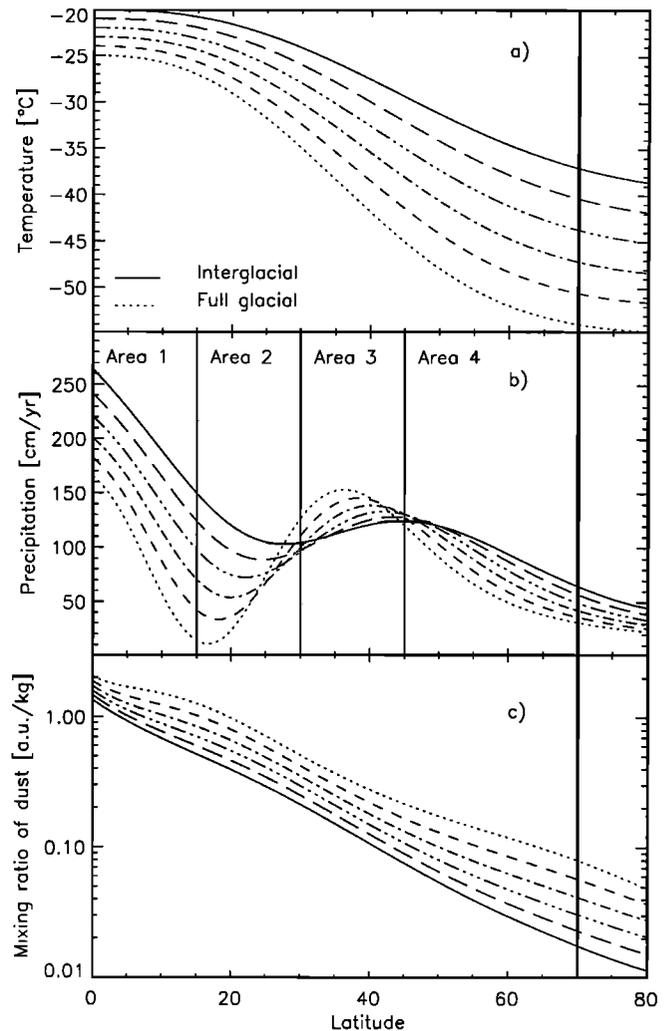

Figure 1. Latitudinal atmospheric profiles of (a) temperature, (b) precipitation, and (c) atmospheric mixing ratio of dust corresponding to the different climatic scenarios in the model. The solid curves correspond to present-day conditions, and the dotted curves correspond to full glacial conditions. Dashed curves in between correspond to intermediate conditions. The bold vertical line indicates $\phi = 70°$, and the thin vertical lines in Figure 1b indicate the location of areas 1-4.

$$\frac{\partial x}{\partial t} - \frac{1}{a^2}\frac{\partial}{\partial\mu}(-k\frac{\partial x}{\partial\mu}(1 - \mu^2)) = x_{\rm in} - x_{\rm out}. \quad (1)$$

This dynamic equation applies for moisture, $q(\mu,t)$, as well as dust, $c(\mu,t)$, with the terms on the right-hand side being specific for the two species. The position of the maximum temperature gradient is the baroclinic zone, in which the poleward transport of moist air is at a maximum. Thus the physics described by the diffusion is the baroclinic transportation. The value of k' is 1×10^{12} m²/d consistent with *Wiin-Nielsen* [1988].

The first term on the right-hand side is the prescribed evaporation $q_{\rm in}$, or dust uptake $c_{\rm in}$. These input functions are chosen to be of the form

$$x_{\text{in}} = x_0 \exp(-\frac{\phi}{\gamma_x}) \qquad (2)$$

For x_{in} being the evaporation, γ_q is equal to 40°, and the maximum flux x_0 is proportional to the saturated moisture content q_{sat} of the air at $\phi_{\text{evap}} = 15°$. The constants were determined by comparison of the resulting latitudinal variations of atmospheric humidity and evaporation-precipitation with climatic data of the present atmosphere [*Peixeto and Oort*, 1992]. This formulation makes the evaporation dependent on the variation of the subtropical temperature but not on the exact form of the temperature profile.

As the aim of this study is to evaluate the influence of a changed atmospheric circulation on dust transportation, dust uptake is taken to be independent of glaciation. The maximum value of the dust input curve, c_0, is set to 1 arbitrary unit (au) per day. The exponential form is adjusted such that the resulting atmospheric mixing ratio of dust at low latitudes is 2 orders of magnitude higher than at high latitudes, as inferred from present-day observations [*Duce*, 1994; *Prospero*, 1996]. This implies $\gamma_c = 10°$.

The exponential form of the input curves is certainly very simplified, but it supplies a constant source of moisture and dust from the lowest latitudes. Furthermore, it facilitates the apprehension of the competing processes of transport and washout. Section 3.3 describes an experiment where the input function for dust was separated into four distinct latitudinal bands. This allows an estimation of the behavior of the model for more realistic source areas of dust.

The precipitation q_{out} is calculated from

$$q_{\text{out}} = \max(0, \frac{q - \lambda q_{\text{sat}}(T)}{\tau}), \qquad (3)$$

where $\lambda = 0.5$ as determined by comparison of the relative humidity with present climatology [*Peixeto and Oort*, 1992]. The time constant of the formation of precipitation, τ, is taken to be 0.1 day, but the model is rather insensitive to the exact value of τ.

Wet deposition of dust is parametrized following *Genthon* [1992] :

$$c_{\text{out}} = c[1 - \exp(-\alpha Q_{\text{out}}dt)]/dt \qquad (4)$$

where c is the atmospheric mixing ratio of dust and α is a scavenging coefficient equal to 0.1 m^2/kg. Q_{out} is the total flux of precipitation to the ground at a given latitude. From the results for c_{out} and q_{out} the concentration of dust in precipitation is calculated as conc $= c_{\text{out}}/q_{\text{out}}$. The model only accounts for wet deposition, and there is no estimation of the influence of an altered climate on dry deposition. Furthermore, the model only describes large-scale precipitation from baroclinic lifting and does not account for convective processes. This implies that the hydrology of the tropics is not reproduced realistically.

3. Results and Discussion

The model reproduces the present-day zonally averaged hydrological cycle of the northern hemisphere rather well (Figure 1b, solid line). In addition, it shows a halving of precipitation at high latitudes between IG and FG, comparable to what is found from ice core data (Figure 2).

The simulation of dust transportation in the model is compared here with data obtained from the GRIP ice core, where the concentration of Cl^- and insoluble dust has been measured at high resolution over selected intervals within the last glacial cycle. A scatterplot of the concentration of Cl^-, a proxy for maritime aerosols,
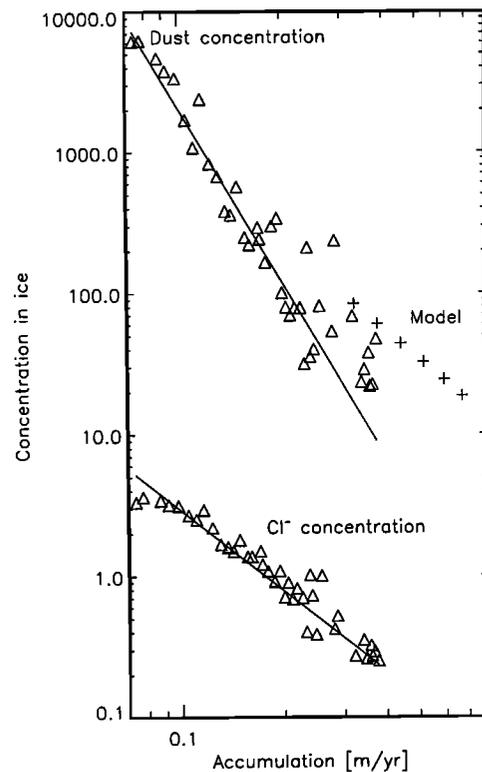
Figure 2. Comparison of the modeled concentration of impurity in the ice at $\phi = 70°$ as a function of precipitation (plus signs). The modeled values are compared with measurements of Cl^- (in $\mu eq/kg$) and continental dust (in $\mu g/kg$) obtained from the Greenland Ice Core Project ice core (triangles) [*De Angelis et al.*, 1997; *Steffensen*, 1997]. The actual measured data set has been reduced by averaging first over 55-cm-length intervals and then over 50 evenly distributed accumulation bins. The first averaging eliminates single measurements with extreme values of $\delta^{18}O$, and we obtain a picture of the general long-term trend. The accumulation (acc) was calculated from the $\delta^{18}O$ isotope ratio, through the relation acc $= 0.23 \times exp(0.14(\delta^{18}O+35.2))$ m/yr [*Dansgaard et al.*, 1993]. Although this is a somewhat simplified relationship [*Kapsner et al.*, 1995], we assume that it is valid for the purpose of these long-term considerations. Overlain on the data are curves with powers β of 1.9 and 4.1.

and continental dust shows approximately a power law relation between accumulation and impurity concentration, concentration $\propto$ accumulation$^{-\beta}$, where the power β is approximately 1.9 for the maritime aerosols and 4.1 for the continental dust (Figure 2). Although both impurities show this power law behavior, the difference in the power suggests that over a glacial cycle different mechanisms for the loading of aerosol into the ice dominate for the two types of aerosol. This is consistent with earlier findings of *Mayewski et al.* [1994].

Dust concentration and precipitation at 70° latitude (corresponding to the summit of the Greenland ice sheet) show negative correlation for the equilibrium solutions to the model (Figure 2). This is a consequence of the prescribed changes in (1) strength and position of the baroclinic zone and (2) evaporation due to the changes in tropical temperatures. In the glacial atmosphere the computed precipitation is reduced and concentrated in the baroclinic zone (Figure 1b) such that the washout of dust becomes less efficient and atmospheric dust "survives" for longer time. This is referred to in the following as the hydrological mechanism. In the model the mixing ratio of dust in the FG atmosphere is generally increased as compared with the warm IG atmosphere. This increase varies with latitude from a factor of 1.5 at the equator to a factor of 5 close to the pole (Figure 1c).

Besides showing an increased transportation of impurities to high latitudes for glacial climates, the model reproduces the power law dependence found between the measured concentration of impurities in the ice and precipitation (Figure 2). The model as described here results in a dependency with a power of $\beta \approx 2$ and an increase in dust concentration from IG to FG conditions by a factor of 4.5 (Table 1). The modeled precipitation as plotted in Figure 2 is somewhat higher than the accumulation obtained from ice core data. However, the model does not account for orographic effects. As may be seen from a precipitation map for Greenland [*Ohmura and Reeh*, 1991], the excess in precipitation

corresponds quite well to the difference in precipitation rate between the summit of the ice sheet and coastal stations.

3.1. Robustness of the Model

The efficacy of the modeled hydrological mechanism depends to varying degrees on the values chosen for the different parameters. The results of an investigation of these dependencies are presented in Table 1.

The input curve for dust, c_{in}, in the model is rather empirical, and the power β is very dependent on the shape of the input curve, with, for example $\gamma_c = 5°$ resulting in $\beta \approx 4$ and an 18-fold increase of dust concentration in the ice at $\phi = 70°$. With this value of γ_c in the model a low- to high-latitude ratio in mixing ratio of 10^3 is produced for the corresponding aerosol.

Another parameter having a significant influence on the hydrological mechanism is the scavenging coefficient α. As may be seen in the work of *Genthon* [1992], the exact value of α depends on (1) the type of scavenging (nucleation or collision), (2) the state of the involved precipitation (liquid or solid), and (3) the size of the involved particles. Since this model gives no estimation for the first two factors, we chose an intermediate value corresponding to particles with a radius representative of long-range transported particles ($r = 1\mu m$), i.e., $\alpha = 0.1$ m^2/kg. The robustness of the model toward a variation of this parameter was tested. Setting $\alpha = 0.5$ m^2/kg implies a stronger scavenging of particles, such that washout of dust generally exceeds transportation. Consequently, especially at high latitudes, the washout is dictated by the prescribed input of dust, which does not change during climate variations in this model. As seen in Table 1 this produces a value of β close to 0. For lower values of α, for example, $\alpha = 0.02$ m^2/kg, the washout of particles becomes less efficient. This results in generally higher atmospheric dust contents, and the low- to high-latitude ratios are decreased due to the diffusion process. Since precipitation is unaffected by the value of α, the washout of dust for different values of α varies concurrently with the atmospheric dust content c. The difference in high-latitude atmospheric dust content between the different climatic scenarios is coupled to the efficiency of washout, implying a greater difference for a higher α. A relatively higher α will thus produce a higher β. In this way the efficacy of the hydrological mechanism is very dependent on the balance between washout and transportation of particles such that both very high and very low values of α actually decrease the value of β. The parameter variations of γ_c and α described above only affect the aerosol transportation and not the hydrological cycle as such.

Changing the difference in pole temperature between IG and FG periods mainly implies a redistribution of precipitation across the baroclinic zone, since the direct influence on q_{in} (through the temperature at ϕ_{evap}) as on q_{sat} is minor. As can be seen from Table 1 the consequence is a very small change in precipitation ($q_{out,FG}/q_{out,IG}$) at $\phi = 70°$ with an in-

Table 1. Results of Sensitivity Tests for $\phi = 70°$

	β	$q_{out,FG}/q_{out,IG}$	Conc$_{FG}$/Conc$_{IG}$
Control	2.06	0.48	4.50
$\gamma_c = 5°C$	3.97	0.48	18.09
$\alpha = 0.02$m^2/kg	1.48	0.48	2.96
$\alpha = 0.5$m^2/kg	1.14	0.48	2.30
$\Delta T_{\phi=80°} = 10°C$	1.75	0.49	3.49
$\Delta T_{\phi=80°} = 22°C$	2.43	0.47	6.38
$\Delta T_{\phi=0°} = 0°C$	2.41	0.73	2.11
$\phi_{evap} = 5°C$	2.04	0.50	4.11
$\phi_{evap} = 25°C$	2.12	0.44	5.84

Corresponding values for the control run are $\gamma_c = 10°$, $\Delta T_{\phi=80°} = 15°C$, $\Delta T_{\phi=0°} = 5°C$, $\phi_{evap} = 15°$, and $\alpha = 0.1$ m^2/kg (Δ=Difference between the IG and the FG value). Abbrevations are FG, full glacial; IG, interglacial; and conc, concentration.

creased/decreased concentration of dust in the ice for the higher/lower temperature difference, i.e., for the stronger/weaker baroclinic zone. However, imposing $\Delta T_{\phi=80°} = 22°C$ (see Table 1 for notation) produces a somewhat unrealistic zone, with $q_{out} = 0$ at low latitudes ($10° \leq \phi \leq 20°$).

Leaving the equator temperature unchanged between IG and FG conditions ($\Delta T_{\phi=0°} = 0°C$) produces about equally high evaporation for the different climate conditions, such that the main effect of the hydrological mechanism is through a redistribution of precipitation over the baroclinic zone, with the total amount of precipitation being unaltered. The result is an almost unchanged β, but with q_{out} and c_{out} varying over much smaller ranges than for the control run.

Similarly, it may be seen that the effect of changing ϕ_{evap} is to alter the total moisture content of the model and with that the total washout of dust. Accordingly, β remains close to constant, with the value ranges for q_{out} and c_{out} varying.

To sum up, this shows that the hydrological mechanism is robust to most of the chosen parameters, with the main control being exerted through γ_c and α. In this way our model suggests that the hydrological mechanism described here may account for a twofold to 18-fold increase in impurity concentration at $\phi = 70°$.

3.2. The Relative Importance of Transportation Versus Washout

Two competing processes determine the effectiveness the hydrological mechanism. These processes are (1) transportation and (2) washout of particles. The relative importance of these processes changes between different latitudinal bands, as illustrated through a box diagram shown in Figure 3.

In order to elucidate the importance of these processes we summed the washout and transportation of dust particles over the areas indicated in Figure 1b.
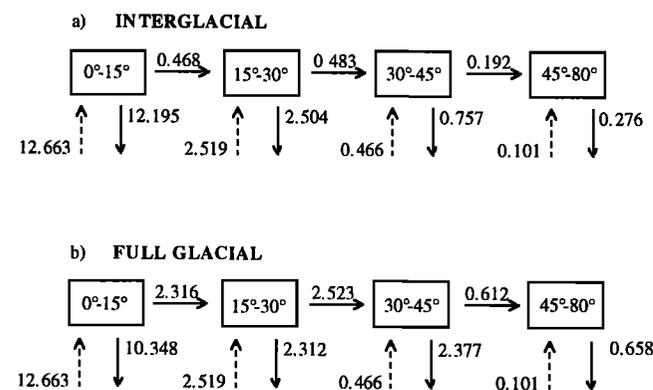
a) INTERGLACIAL

$$\boxed{0°\text{-}15°} \xrightarrow{0.468} \boxed{15°\text{-}30°} \xrightarrow{0.483} \boxed{30°\text{-}45°} \xrightarrow{0.192} \boxed{45°\text{-}80°}$$

12.663 ↑ / ↓12.195   ↑ / ↓2.504   2.519 ↑ / ↓0.757   0.466 ↑ / ↓0.276   0.101 ↓

b) FULL GLACIAL

$$\boxed{0°\text{-}15°} \xrightarrow{2.316} \boxed{15°\text{-}30°} \xrightarrow{2.523} \boxed{30°\text{-}45°} \xrightarrow{0.612} \boxed{45°\text{-}80°}$$

12.663 ↑ / ↓10.348   ↑ / ↓2.312   2.519 ↑ / ↓2.377   0.466 ↑ / ↓2.377   0.658 ↓ / 0.101

Figure 3. Box diagram illustrating the relative importance of transportation and washout for area 1 to area 4 (defined in Figure 1b). The numbers are dust fluxes into, out of, and between the areas. Horizontal arrows indicate transportation between the areas, upward arrows indicate uplift of dust, and downward arrows indicate washout of dust.

These areas were chosen according to the characteristics of the hydrological cycle in the following way:

1. Area 1 is the area between the equator and $\phi = 15°$. This is an area where precipitation decreases with latitude and where IG precipitation is higher than FG precipitation.

2. Area 2, the area between $\phi = 15°$ and $\phi = 30°$, contains the precipitation minima for all climate conditions. Again, precipitation is highest for IG conditions.

3. Area 3 ($30° \leq \phi \leq 45°$) contains the precipitation maxima for all periods, i.e., the main part of the baroclinic zone. As a result of the stronger baroclinic zone for glacial conditions this is the only area where FG precipitation exceeds IG precipitation.

4. Area 4 is the area poleward of $45°$. Precipitation decreases monotonously with latitude, being highest for IG conditions.

Returning to Figure 3, it should be kept in mind that the areas are only of approximately equal sizes, as they were chosen from a hydrological point of view. Areas 1-4 contain 24, 22, 18, and 26 latitudinal bands, respectively, of equal sizes. They are thus appropriate for comparison of the magnitude of the different processes for each area and of changes in between the climatic scenarios. However, comparison of values in between the different areas should be done with caution. Keeping this in mind, it may be noted by looking at Figure 3a that for IG conditions both transportation and washout decrease monotonously with latitude, when the input is prescribed by c_{in} as described in section 2. Washout exceeds transportation out of areas 1, 2 and, 3 by decreasing factors of 25.9, 5.2, and 3.9, implying that transportation becomes relatively more important as the baroclinic zone is approached. For FG conditions (Figure 3b), washout and transportation again decrease with increasing latitude, but with local maxima for area 3 and between area 2 and 3. This is anticipated as a consequence of the strengthening and equatorward movement of the baroclinic zone. Again, washout is mostly stronger than transportation out of the areas, with the exception that transportation out of area 2 is actually stronger than washout. This results in ratios of washout over transportation of 4.47, 0.91, and 3.88.

The factors noted above show that at low to middle latitudes the relative importance of transportation as compared with washout increases greatly when going from IG to FG conditions. In fact, transportation increases by factors of 3-5, lowest between the areas closest to the pole. This is a consequence of the equatorward movement of the baroclinic zone. Washout of dust from the areas decreases weakly for the two first areas and increases by a factor of 3 for area 3. These changes may all be ascribed to the changed precipitation in these areas. However, as a consequence of the highly increased atmospheric dust content, washout from area 4 increases by a factor of 2.3 despite a decrease in precipitation by 0.75 (not shown). It may be concluded that between IG and FG conditions, atmospheric transportation of impurities increases largely at

all latitudes, with the washout decreasing at low latitudes and increasing at high latitudes.

3.3. Location of the Aerosol Sources

Biscaye et al. [1997] showed that for the LGM the source areas of dust found at the summit of the Greenland ice sheet were most likely east Asian deserts. Such midlatitude sources are particularly sensitive to the hydrological mechanism since their location relative to the baroclinic zone may change considerably in the course of climate variations. Washout of dust on the way from sources poleward of the baroclinic zone is considerably weaker than for sources farther equatorward. Moreover, a change in the location of source areas with time could influence the effect of the hydrological mechanism considerably. Enhanced loess accumulation, short-range dust transportation, for example [*Pye*, 1987], a generally increased aridity [*Sarnthein*, 1978], as well as higher wind speeds, are all indications of higher dust production during the LGM.

In order to test the effect of the hydrological mechanism on dust deriving from sources at different latitudinal locations, we have split the general source function of dust c_{in} into four independent areas. As the model is linear in terms of dust, this amounts to the same total curves as discussed earlier.

The location of the different areas was chosen from the behavior of the hydrological cycle as explained in section 3.2. As mentioned earlier the exponential form of the input curve is very idealized and was mainly chosen for the sake of simplicity. However, when splitting the curve into the four distinct areas, the following may be noted:

1. Area 1 for both hemispheres contains mostly tropical areas and very few potential dust sources. It will not be included in further discussion of sources of long-range transported dust.

2. Area 2 for the northern hemisphere contains most of the African and Arabian sources of eolian dust. For the southern hemisphere it contains source areas in Africa and Australia.

3. Area 3 contains mainly source areas in Asia and North America for the northern hemisphere and in South America for the southern hemisphere. This area includes the most likely sources of dust transported both to Greenland [*Biscaye et al.*, 1997] and to Antarctica [*Basile et al.*, 1997] during the LGM.

4. Area 4 contains very few source areas of dust for the present-day climate, but it includes shelf areas at high latitudes, which were exposed during the LGM and which may have been possible sources of eolian dust.

In area 2, washout close to the source area is highest for IG, and since the total amount of precipitation is decreased for FG this amounts to highest concentrations of dust from this area for FG at all latitudes (see Figure 4). For area 3 ($30° \leq \phi \leq 45°$), washout close to the sources is highest for FG conditions, but it is highest for IG conditions poleward of the source area, inferring highest concentrations close to the source areas for IG
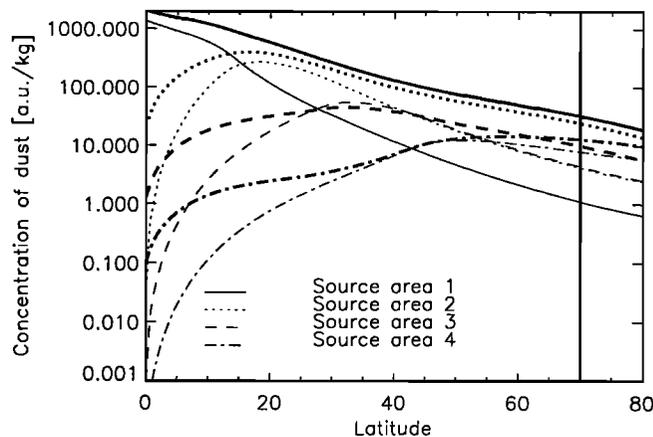

Figure 4. Resulting latitudinal profiles of the concentration of dust in precipitation, when the sources are split into four areas. Results are presented for interglacial (thin curves) and full glacial (bold curves) conditions. The bold vertical line indicates $\phi = 70°$.

conditions, but for FG conditions everywhere else. For source area 4 (poleward of 45°), precipitation is highest during IG, such that most dust is washed out over the sources during IG, with resulting lowest concentrations for these conditions. To sum up, the hydrological mechanism is most effective for sources areas close to the equator with decreasing effectivity poleward. However, the effect of the mechanism at midlatitudes is very dependent on the exact location of the sources.

Regarding the concentration of dust in the ice at $\phi = 70°$, it is seen (Figure 4) that the increase from FG to IG is stronger, the farther equatorward the source area of the dust is. However, since there are only few potential sources of dust transported to polar ice caps in area 1, the strong increase found for dust from this area is rather unrealistic. The concentration of dust from area 2 increases by a factor of 6, whereas the concentration of dust from area 3 only increases by a factor of 2.

Deep-sea sediment cores provide a long-term record of transportation of eolian material. They generally indicate that the amount of dust transported in the northern hemisphere may have been 3-5 times higher during glacial times than now [*Rea*, 1994]. During recent years several, low- to middle-latitude ice cores have been drilled. They, too, provide evidence of increased amounts of eolian dust at these latitudes during glacial periods. In an ice core taken from the Dunde ice cap in China [*Thompson et al.*, 1990], a fourfold to eightfold fold increase in dust concentration from IG to FG conditions was found. Another Asian ice core from the Guliya ice cap on the Qinghai-Tibetan Plateau [*Thompson et al.*, 1997] shows increased dust levels in glacial ice of about a factor 100 higher than in interglacial ice. A corresponding increase of about 200 is found in two tropical ice cores from Huascarán, Peru [*Thompson et al.*, 1995].

When investigating the corresponding results from the model (Figure 4), it is found that the concentration of dust from low-latitude sources (area 1) increases only by a factor of about 2 at $\phi = 10°$ (approximately the location of the Peruvian cores). However, as earlier mentioned, the tropics are not necessarily realistically simulated in this model. For $\phi = 40°$ (corresponding to the Asian ice cores), we find an increase in concentration by a factor of 10 for dust from source area 1, by a factor of 4 from area 2, and by a factor close to 0 for dust from the other areas. This may correspond to the overall increase found from ocean cores as well as the increase found in the Dunde ice cap, but the increase found in the Guliya ice cap is certainly not reproduced. A possible explanation may be that this ice cap is in relative proximity of potential source areas, and local features which are not captured by this model may play a significant role.

3.4. Sea Salt

Assuming that the global ocean sources of sea salt transported to high latitudes did not change considerably over the last glacial cycle, it is plausible that (to a first approximation) the hydrological mechanism taken together with an increased uptake due to higher wind speeds accounts for the whole change in maritime aerosol load in the ice core. Owing to the higher scavenging ratio for hygroscopic sea salt, resulting in a smaller β, the results of this model are somewhat exaggerated when applied to sea salt. In this way the value of $\beta = 2.0$ produced by the model fits very well with the increase found for the marine aerosol (Cl^-) in the GRIP ice core ($\beta = 1.9$).

4. Conclusions

From the hydrological mechanism described by our model we can reproduce the power law dependence between the concentration of aerosols in polar ice and snow accumulation, which is observed for both maritime and terrestrial aerosols. The power obtained in the model depends on the exact form of the input curve of the aerosol, i.e., on the location of the sources relative to the baroclinic zone. In this model, strength and location of the aerosol sources do not change with climate. Assuming that the input of aerosols to the atmosphere decreases exponentially with latitude and using reasonable estimates for the parameters in the model, the hydrological mechanism in the model may account for a twofold to 18-fold increase in the concentration of an impurity found in polar ice cores. In this way the hydrological mechanism can explain most of the increase observed for maritime aerosols. However, when taking into account the location of realistic source areas of dust transported to polar ice caps, it appears that the hydrological mechanism probably only accounts for a factor of between 2 and 6 of the observed 100-fold increase. The model simulates increased atmospheric dust contents for the glacial climate by a factor of up to

5, but the very high increase in dust concentrations that have been reported from some low- to middle-latitude ice cores cannot be reproduced.

This implies that although the hydrological mechanism as simulated here may have a significant influence on the increased dust amounts found in polar ice caps during glacial periods, other factors must be at least equally important. In this simplified 1-D model we have not attempted to evaluate the effect of higher wind speeds during glacial periods on the uplift of dust, nor can we account for changes in zonal transportation, which may be quite significant due to, for example, the waxing of the Laurentide ice sheet. These factors together with possible changes in the exact source extents and locations will have to be investigated with more complex models such as GCMs.

References

Andersen, K. K., and C. Genthon, Modeling the present and last glacial maximum transportation of dust to the Arctic with an extended source scheme, in *The Impact of Desert Dust Across the Mediterranean*, edited by S. Guerzoni and R. Chester, pp. 123–132, Kluwer Acad., Norwell, Mass., 1996.

Basile, I., F. E. Grousset, M. Revel, J. R. Petit, P. E. Biscaye, and N. I. Barkov, Patagonian origin of glacial dust deposited in east Antarctica (Vostok and Dome C) during glacial stages 2, 4 and 6, *Earth Planet. Sci. Lett.*, *146*, 573–589, 1997.

Biscaye, P. E., F. E. Grousset, M. Revel, S. Van der Gaast, G. A. Zielinski, A. Vaars, and G. Kukla, Asian provenance of glacial dust (stage 2) in the Greenland Ice Sheet Project 2 ice core, Summit, Greenland, *J. Geophys. Res.*, *102*, 26,765–26,781, 1997.

Dansgaard, W., et al., Evidence for general instability of past climate from a 250-kyr ice-core record, *Nature*, *364*, 218–220, 1993.

De Angelis, M., J. P. Steffensen, M. Legrand, H. B. Clausen, and C. Hammer, Primary aerosol (sea salt and soil dust) deposited in Greenland ice during the last climatic cycle: Comparison with east Antarctic records, *J. Geophys. Res.*, *102*, 26,681–26,698, 1997.

Ditlevsen, P. D., H. Svensmark, and S. Johnsen, Contrasting atmospheric and climate dynamics of the last-glacial and Holocene periods, *Nature*, *379*, 810–812, 1996.

Duce, R., Sources, distributions, and fluxes of mineral aerosols and their relationship to climate, In *Aerosol Forcing of Climate*, edited by R. J. Charlson and J. Heintzenberg, pp. 43–72, John Wiley, New York, 1994.

Genthon, C., Simulations of desert dust and sea-salt aerosols in Antarctica with a general circulation model of the atmosphere, *Tellus, Ser. B*, *44*, 371–389, 1992.

Greenland Ice Core Project members, Climate instability during the last interglacial period recorded in the GRIP ice core, *Nature*, *364*, 203–207, 1993.

Guilderson, T., R. G. Fairbanks, and J. L. Rubenstone,

Tropical temperature variations since 20,000 years ago: modulating interhemispheric climate change, *Science*, *263*, 663–665, 1994.

Hammer, C. U., H. B. Clausen, W. Dansgaard, A. Neftel, P. Kristinsdottir, and E. Johnson, Continuous impurity analysis along the Dye 3 deep core, In *Greenland Ice Core: Geophysics, Geochemistry, and the Environment*, *Geophys. Monogr. Ser.*, vol. 33, edited by C. C. Langway, H. Oeschger, and W. Dansgaard, pp. 90–94, AGU, Washington, D. C., 1985.

Hansson, M. E., Are changes in atmospheric cleansing responsible for observed variations of impurity concentrations in ice cores?, *Ann. Glaciol.*, *21*, 219–224, 1995.

Johnsen, S. J., H. B. Clausen, W. Dansgaard, K. Fuhrer, N. Gundestrup, C. U. Hammer, P. Iversen, J. Jouzel, B. Stauffer, and J. P. Steffensen, Irregular glacial interstadials recorded in a new Greenland ice core, *Nature*, *359*, 311–313, 1992.

Johnsen, S., D. Dahl-Jensen, W. Dansgaard, and N. Gundestrup, Greenland paleotemperatures derived from GRIP bore hole temperature and ice core isotopic profiles, *Tellus, Ser. B, 47*, 624–629, 1995.

Joussaume, S., Paleoclimatic tracers: An investigation using an atmospheric general circulation model under ice age conditions, 1, Desert dust, *J. Geophys. Res.*, *98*, 2767–2805, 1993.

Kapsner, W., R. Alley, C. Shuman, S. Anandakrishnan, and P. Grootes, Dominant influence of atmospheric circulation on snow accumulation in Greenland over the past 18,000 years, *Nature*, *373*, 52–54, 1995.

Kutzbach, J. E., and H. E. Wright Jr., Simulation of the climate of 18,000 years BP: Results for the North American/North Atlantic/European sector and comparison with the geologic record of North America, *Quat. Sci. Rev.*, *4*, 147–187, 1985.

Marsh, N. D., and P. D. Ditlevsen, Observation of atmospheric and climate dynamics from a high-resolution ice core record of a passive tracer over the last glaciation, *J. Geophys. Res.*, *102*, 11,219–11,224, 1997.

Mayewski, P. A., et al., Changes in atmospheric circulation and ocean ice cover over the north Atlantic during the last 41,000 years, *Science*, *263*, 1747–1751, 1994.

Ohmura, A., and N. Reeh, New precipitation and accumulation maps for Greenland, *J. Glaciol.*, *37*, 140–148, 1991.

Peixeto, J. P., and A. H. Oort, *Physics of Climate*, Am. Inst. of Phys., New York, 1992.

Petit, J., M. Briat, and A. Royer, Ice age aerosol content from east Antarctic ice core samples and past wind strength, *Nature*, *293*, 391–394, 1981.

Prospero, J. M., Saharan dust transport over the North Atlantic Ocean and Mediterranean: An overview, in *The Impact of Desert Dust Across the Mediterranean*, edited by S. Guerzoni and R. Chester, pp. 133–153, Kluwer Acad., Norwell, Mass., 1996.

Pye, K., *Aeolian Dust and Dust Deposits*, Academic, San Diego, Calif., 1987.

Rea, D. K., The paleoclimatic record provided by eolian deposition in the deep sea: The geologic history of wind, *Rev. Geophys.*, *32*, 159–195, 1994.

Sarnthein, M., Sand deserts during glacial maximum and climatic optimum, *Nature*, *272*, 43–46, 1978.

Steffensen, J. P., The size distribution of microparticles from selected segments of the Greenland Ice Core Project ice core representing different climatic periods, *J. Geophys. Res.*, *102*, (C12), 26,755–26,763, 1997.

Thompson, L. G., and E. Mosley-Thompson, Microparticle concentration variations linked with climatic change: Evidence from polar ice cores, *Science*, *212*, 812–815, 1981.

Thompson, L. G., E. Mosley-Thompson, M. E. Davis, J. Bolzan, J. Dai, and L. Klein, Glacial stage ice-core records from the subtropical Dunde ice cap, China, *Ann. Glaciol.*, *14*, 288–297, 1990.

Thompson, L. G., E. Mosley-Thompson, M. E. Davis, P.-N. Lin, K. A. Henderson, J. Cole-Dai, J. F. Bolzan, and K.-B. Liu, Late glacial stage and Holocene tropical ice core records from Huascarán, Peru, *Science*, *269*, 46–50, 1995.

Thompson, L., T. Yao, M. Davis, K. Henderson, E. Mosley-Thompson, P.-N. Lin, J. Beer, H.-A. Synal, J. Cole-Dai, and J. Bolzan, Tropical climate instability: The last glacial cycle from a Qinghai-Tibetan ice core, *Science*, *276*, 1821–1825, 1997.

Wiin-Nielsen, A., A heuristic theory of the zonally-averaged state of the atmosphere, *Mat. Fys. Medd. K. Dan. Vidensk. Selsk.*, *42:2*, 1988.

Yung, Y., T. Lee, C.-H. Wang, and Y.-T. Shieh, Dust: A diagnostic of the hydrological cycle during the last glacial maximum, *Science*, *271*, 962–963, 1996.

K. K. Andersen and P. D. Ditlevsen, Department of Geophysics, Niels Bohr Institute, University of Copenhagen, Juliane Maries Vej 30, DK-2100 Copenhagen OE, Denmark. e-mail: kka@gfy.ku.dk; pditlev@gfy.ku.dk)